Predicting Antibody Responses to Type V GBS-TT Conjugate Vaccine Using Computational Modelling

Matheus R. Ribeiro[1], Bárbara de M. Quintela[2[0000−0002−5320−4109]], Ruy F. Reis[2[0000−0001−5215−3744]], Rodrigo W. dos Santos[2[0000−0002−0633−1391]], and Marcelo Lobosco[2[0000−0002−7205−9509]]

[1] Computational Engineering, Federal University of Juiz de Fora, Juiz de Fora, 36038-330, Brazil
matheus.reis@estudante.ufjf.br

[2] Graduate Program in Computational Modelling, Federal University of Juiz de Fora, Juiz de Fora, 36038-330, Brazil
{barbara.quintela,ruy.reis,rodrigo.weber,marcelo.lobosco}@ufjf.br

Abstract. Group B Streptococcus (GBS) remains a leading cause of neonatal mortality, underscoring the need for effective vaccination strategies. This study introduces a novel adaptation of an ODE-based immunological model to simulate the response to a Type V GBS-TT conjugate vaccine, with model calibration and validation performed against clinical data. Utilizing Differential Evolution, we accurately estimated immunological parameters across various dosages, revealing mechanistic differences between conjugated and unconjugated formulations. Our numerical results show that key parameters — specifically, the antigen-presenting cell maturation rate and the antibody-mediated vaccine clearance rate — were 93-fold and 1,700-fold higher, respectively, in conjugated vaccines compared to unconjugated formulations. These findings underscore the adjuvant effect of tetanus toxoid and demonstrate the model's capacity for guiding rational vaccine design and optimization.

Keywords: Computational Immunology · Computational Vaccinology · Computational Modelling · Group B Streptococcus

1 Introduction

Group B Streptococcus (GBS), scientifically known as *Streptococcus agalactiae*, is a bacterium commonly found in the gastrointestinal and genital tracts of healthy individuals. Although typically asymptomatic in adults, GBS can cause severe infections, particularly in newborns and immunocompromised individuals. It remains a leading cause of neonatal morbidity and mortality [11]. In newborns, GBS infections often result in life-threatening conditions such as sepsis, pneumonia, and meningitis. Early-onset disease (EOD), which manifests within the first 6 days of life, accounts for approximately 60–70% of neonatal GBS cases, usually transmitted vertically during childbirth via aspiration of infected fluids.

ICCS Camera Ready Version 2025
To cite this paper please use the final published version:
DOI: 10.1007/978-3-031-97554-7_27

Globally, approximately 18% [17] to 23% [8] of pregnant women are GBS carriers. In contrast, late-onset disease (LOD), occurring between the first week and up to 90 days of life, is associated with alternative transmission routes, such as breast milk, nosocomial exposure, or community exposure [12]. Annually, GBS infections are estimated to cause 410,000 cases worldwide, leading to 147,000 stillbirths and infant deaths, with the highest burden observed in Africa [18].

In adults, GBS infections can manifest as urinary tract infections, skin and soft tissue infections, and, less frequently, bloodstream infections and meningitis, with higher risks among individuals with predisposing conditions such as diabetes or chronic kidney disease.

The most widely used strategy to prevent GBS disease involves screening pregnant women between 35 and 37 weeks of gestation for GBS colonization, followed by administering intravenous antimicrobial prophylaxis (IAP) during labour [12]. Additionally, the transplacental transfer of immunoglobulin G (IgG) antibodies specific to *S. agalactiae* renders maternal vaccination a promising strategy to protect mothers, fetuses, and newborns. Vaccinating mothers in the late second or early third trimester could effectively reduce GBS disease in both mothers and infants [8]. *S. agalactiae* is classified into ten serotypes [16], with dominant serotypes varying by region. This variation emphasizes the need for conjugate vaccines targeting multiple serotypes. The development of the Type V GBS-TT conjugate vaccine represents a significant milestone in preventing invasive GBS disease [1], despite challenges in manufacturing and high costs [14]. Nonetheless, critical questions remain regarding the vaccine's long-term efficacy, optimal usage strategies, immunogenicity across diverse populations, and safety profile. For instance, the duration of immunity conferred by the vaccine is not fully understood, raising concerns about the need for booster doses, particularly in immunocompromised populations.

Furthermore, determining the optimal timing for vaccination during pregnancy to ensure maximal neonatal protection is essential. Additional research is also required to assess whether the GBS-TT conjugate vaccine can be safely and effectively co-administered with other vaccines in both single-dose and multi-dose regimens. Addressing these gaps is vital to fully harnessing the benefits of the Type V GBS-TT conjugate vaccine.

Computational models have emerged as valuable tools in vaccine research by simulating disease dynamics, immune responses, and vaccine effects in a controlled virtual environment. These models, which employ mathematical equations, statistical methods, and computer simulations, replicate biological processes and predict vaccine performance under various conditions. They can supplement, or in some cases replace, traditional clinical trials when ethical, practical, or financial constraints limit conventional testing. Specifically, computational models enable rapid exploration of multiple scenarios—such as evaluating different vaccine dosages, schedules, or combinations—without the time and cost associated with clinical trials, thereby allowing researchers to test hypotheses and refine protocols before advancing to animal or human studies [4].

ICCS Camera Ready Version 2025
To cite this paper please use the final published version:
DOI: 10.1007/978-3-031-97554-7_27

This study presents results from an *in silico* dose-response experiment designed to reproduce cohort data reported by Baker *et al.* [1]. A pre-existing immune response model [3] was adapted using Differential Evolution to adjust initial conditions and key constants to fit the cohort data for a single dose of the GBS-TT conjugate vaccine [1]. The model was then validated using data from subsequent doses, demonstrating accurate replication across different vaccine dosages.

This paper is organized as follows: Section 2 provides background information on the immune system and the Type V GBS-TT vaccine. Section 3 briefly reviews the relevant literature. Section 4 details the method, including the mathematical model used to simulate the immune response to the GBS-TT conjugate vaccine and the adjustments made to fit the cohort data. Section 5 presents and discusses the numerical results. Finally, Section 6 concludes the study with a summary and suggestions for future research.

2 Background

Once in the body, the innate immune system provides the first line of defence against GBS. Upon infection, pattern recognition receptors (PRRs), such as Toll-like receptors (TLRs) and NOD-like receptors, detect pathogen-associated molecular patterns (PAMPs) on GBS. This recognition triggers the activation of immune cells like neutrophils and macrophages, which phagocytose and destroy the bacteria [20]. Additionally, the innate immune response involves the production of pro-inflammatory cytokines and chemokines, which recruit additional immune cells to the site of infection [20].

The adaptive immune system is activated following the innate response, providing a more targeted defence against GBS. B cells produce specific antibodies against GBS antigens, primarily targeting the polysaccharide capsule, a significant virulence factor of the bacterium. These antibodies facilitate opsonization, thereby enhancing phagocytosis by immune cells [20]. T cells, particularly CD4+ helper T cells, are critical in orchestrating the immune response by secreting cytokines that further activate B cells and macrophages [20].

The immune response elicited by vaccination mimics the natural infection process but in a controlled and safe manner. Vaccines introduce antigens derived from the pathogen, which stimulate the immune system to generate a memory response without causing disease. Upon subsequent exposure to the same pathogen, the immune system can mount a faster and more robust response, preventing infection. GBS has nine capsular polysaccharide serotypes (CPS), Ia, Ib, and II-VIII, each with varying global prevalence [1]. This necessitates a polyvalent GBS conjugate vaccine formulated with the most prevalent serotypes in a specific population to provide broad protection.

A previous study in the literature [1] evaluated the immunogenicity and reactogenicity of Type V GBS-TT conjugate vaccine at different dosages in cohort of healthy adults. The vaccine is prepared with GBS type V stain CBJ111. After growing in a culture, the capsular polysaccharides (CPS) of the bacterium were

ICCS Camera Ready Version 2025
To cite this paper please use the final published version:
DOI: 10.1007/978-3-031-97554-7_27

removed by base extraction followed by chemical treatment [1]. In the case of the Type V GBS-TT conjugate vaccine, CPS is conjugated with tetanus toxoid to increase the immunogenicity of the Type V GBS vaccine. No other adjuvant was used in this process. The study demonstrated that the vaccine effectively elicited a dose-dependent immune response, with higher doses correlating to increased production of specific antibodies against GBS type V polysaccharides as Fig. 1 shows. Moreover, the study reported that the vaccine was well-tolerated, with mild and transient adverse reactions such as injection site pain and low-grade fever. These findings highlight the potential of the Type V GBS-TT vaccine as a preventive strategy against invasive GBS disease.

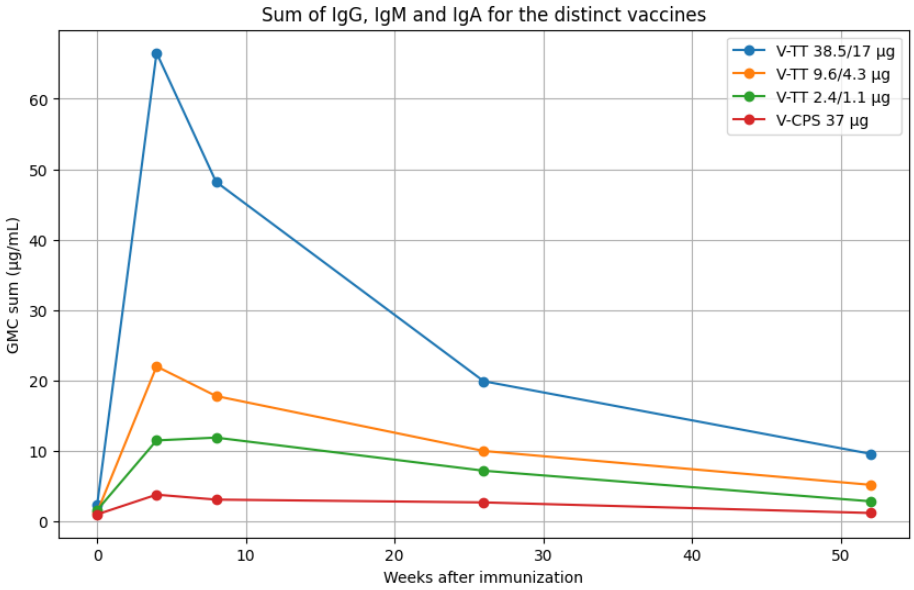

Fig. 1. Production of antibodies for different doses and types of GBS vaccines. The figure shows the sum of the geometric mean concentrations (GMC) of IgG, IgM, and IgA for the V CPS and V–TT vaccines. V CPS is a vaccine that protects against type V GBS using the type V capsular polysaccharide (CPS). V–TT is a conjugate vaccine that combines tetanus toxoid (TT) with CPS. For the V–TT vaccine, different combinations of CPS and TT were used [1].

3 Literature Review

Mathematical and computational modelling are essential tools for analysing the complex dynamics of vaccine-induced immune responses. These approaches integrate immunological mechanisms with population-level effects to predict vaccine efficacy, optimize dosing strategies, and inform clinical trial design [2, 4–6].

ICCS Camera Ready Version 2025
To cite this paper please use the final published version:
DOI: 10.1007/978-3-031-97554-7_27

Different modelling paradigms offer distinct advantages. Discrete agent-based models (ABMs) can capture heterogeneity in immune responses by simulating individual immune cell interactions [7]. An ABM [15] predicted that the citrus-derived compound neohesperidin could enhance the immune response to a vaccine against human papillomavirus.

Recent advances employ machine learning (ML) techniques to predict immunogenicity from vaccine formulation parameters [10]. ML approaches identify B and T cell epitopes and correlates of protection, potentially improving vaccine target selection [5]. The SIMON automated ML system, capable of handling incomplete datasets, has revealed previously unrecognized CD4+ and CD8+ T cell subsets that are strongly associated with robust antibody responses to influenza antigens [22].

Ordinary differential equation (ODE) models are widely employed to describe the temporal dynamics of immune cell populations, antigen levels, and pathogen load following vaccination [3, 9, 23]. These models, typically formulated as systems of nonlinear differential equations, provide a simplified yet informative representation of the immune response. A recent study employed an ODE model to compare antibody dynamics after administering inactivated, mRNA, and attenuated vaccines, highlighted the crucial role of booster shots [23].

While ABMs offer detailed cell-level resolution and ML pipelines can uncover non-obvious correlates of protection, ODE models strike an optimal balance between interpretability and computational efficiency. By enabling direct mapping of clinical time-course data onto mechanistic parameters, they facilitate clear hypothesis testing and rapid *in silico* exploration of dosing regimens. In this study, we extend an established ODE model [3] to the Type V GBS-TT conjugate vaccine context, thereby integrating rigorous mechanistic insight with quantitative calibration against phase 1 cohort data.

Parameter estimation is crucial for calibrating ODE models to experimental data. Various methods exist, ranging from gradient-based optimization techniques, which require sensitivity analysis (like adjoint methods, efficient for large systems), to Bayesian approaches like Markov Chain Monte Carlo (MCMC) that provide uncertainty quantification but can be computationally intensive. ML methods are also emerging for parameter inference in complex systems. Differential Evolution (DE), used in this study, is a stochastic, population-based global optimization heuristic. While perhaps simpler to implement than gradient-based or complex Bayesian methods (as it doesn't require derivative information), DE has proven effective for complex, multi-modal optimization problems common in biological systems. Its application here allows for robust exploration of the parameter space to fit the ODE model to the available clinical data, offering a practical alternative for calibrating this specific immunological model.

The following sections detail the specific ODE model adaptation, the DE method used for parameter calibration against cohort data, and the subsequent validation experiments.

ICCS Camera Ready Version 2025
To cite this paper please use the final published version:
DOI: 10.1007/978-3-031-97554-7_27

4 Methods

4.1 Mathematical Model

The system of ordinary differential equations (ODEs) used to model the immune response to CPS/GBS-TT vaccines was adapted from an earlier study [3]. These equations describe the interactions among vaccine particles (Vp), antigen-presenting cells (naive, Ap, and mature, Apm), lymphocytes (Thn, The, Tkn, Tke, B, Bm, Ps, and Pl), and antibodies (A). The complete system of equations is reproduced here for clarity.

Vaccine Particles: The dynamics of the vaccine population (Vp) are given by:

$$\frac{d}{dt}Vp = -\left(\frac{c_{v1}Vp}{c_{v2}+Vp}\right) - k_{v1}VpA - k_{v2}VpTke, \tag{1}$$

where the first term represents a saturating elimination of vaccine particles, the second term corresponds to vaccine neutralization by antibodies (with rate k_{v1}), and the third term accounts for elimination by effector killer T cells (with rate k_{v2}). Although the second term simplifies the biological process known as opsonization, it is important to note that antibodies mark the vaccine particles for elimination rather than directly eliminating them.

Immature Antigen-Presenting Cells: The dynamics of immature antigen-presenting cells (Ap) are modeled by:

$$\frac{d}{dt}Ap = \alpha_{ap}(Ap_0 - Ap) - \beta_{ap}Ap\left(\frac{c_{ap1}Vp}{c_{ap2}+Vp}\right), \tag{2}$$

where Ap_0 denotes the homeostatic concentration of immature APCs, α_{ap} is the rate at which homeostasis is achieved, and β_{ap} characterizes the maturation of naive APCs upon encountering vaccine particles.

Mature Antigen-Presenting Cells: The dynamics of mature APCs (Apm) are described by:

$$\frac{d}{dt}Apm = \beta_{ap}Ap\left(\frac{c_{ap1}Vp}{c_{ap2}+Vp}\right) - \delta_{apm}Apm, \tag{3}$$

with the first term representing the maturation of APCs from their immature precursors and the second term accounting for the natural decay of mature APCs at rate δ_{apm}.

Naive Helper T Cells: The dynamics of naive helper T cells (Thn) are given by:

$$\frac{d}{dt}Thn = \alpha_{th}(Thn_0 - Thn) - \beta_{th}ApmThn, \tag{4}$$

where Thn_0 is the homeostatic level of naive helper T cells, α_{th} is the homeostasis rate, and β_{th} represents their activation by mature APCs.

Effector Helper T Cells: The dynamics of effector helper T cells (The) are described by:

$$\frac{d}{dt}The = \beta_{th}ApmThn + \pi_{th}ApmThe - \delta_{th}The, \tag{5}$$

ICCS Camera Ready Version 2025
To cite this paper please use the final published version:
DOI: 10.1007/978-3-031-97554-7_27

where the first term represents the activation of helper T cells, the second term models their replication at rate π_{th}, and the third term accounts for their decay at rate δ_{th}.

Naive Killer T Cells: The dynamics of naive killer T cells (Tkn) are described by:

$$\frac{d}{dt}Tkn = \alpha_{tk}(Tkn_0 - Tkn) - \beta_{tk}ApmTkn, \tag{6}$$

with Tkn_0 representing the homeostatic level of naive killer T cells, α_{tk} the homeostasis rate, and β_{tk} their activation rate by mature APCs.

Effector Killer T Cells: The dynamics of effector killer T cells (Tke) are given by:

$$\frac{d}{dt}Tke = \beta_{tk}ApmTkn + \pi_{tk}ApmTke - \delta_{tk}Tke, \tag{7}$$

where the first term represents the activation of naive killer T cells, the second term models their replication at rate π_{tk}, and the third term describes their decay at rate δ_{tk}.

B Lymphocytes: The population of B lymphocytes (B) is modeled as:

$$\frac{d}{dt}B = \alpha_b(B_0 - B) + \pi_{b2}The\,B - \beta_{ps}Apm\,B - \beta_{pl}The\,B - \beta_{bm}The\,B, \tag{8}$$

where B_0 is the homeostatic level of B cells, α_b is the homeostasis rate, $\pi_{b2}The\,B$ represents B cell proliferation stimulated by effector helper T cells, and the terms $\beta_{ps}Apm\,B$, $\beta_{pl}The\,B$, and $\beta_{bm}The\,B$ model the differentiation of B cells into short-lived plasmocytes, long-lived plasmocytes, and memory B cells, respectively.

Memory B Cells: The dynamics of memory B cells (Bm) are represented by:

$$\frac{d}{dt}Bm = \beta_{bm}The\,B + \pi_{bm1}Bm\left(1 - \frac{Bm}{\pi_{bm2}}\right) - \gamma_{bm}Bm, \tag{9}$$

where the first term represents the generation of memory B cells from B lymphocytes (mediated by effector helper T cells), the second term models memory B cell replication at rate π_{bm1} (with a maximum capacity π_{bm2}), and the final term describes their differentiation into long-lived plasmocytes upon re-exposure to the pathogen.

Short-Lived Plasmocytes: The dynamics of short-lived plasmocytes (Ps) are described by:

$$\frac{d}{dt}Ps = \beta_{ps}Apm\,B - \delta_{ps}Ps, \tag{10}$$

where $\beta_{ps}Apm\,B$ represents the production of short-lived plasmocytes from B cells and δ_{ps} is their decay rate.

Long-Lived Plasmocytes: Long-lived plasmocytes (Pl) are modeled by:

$$\frac{d}{dt}Pl = \beta_{pl}The\,B - \delta_{pl}Pl + \gamma_{bm}Bm, \tag{11}$$

ICCS Camera Ready Version 2025
To cite this paper please use the final published version:
DOI: 10.1007/978-3-031-97554-7_27

where the first term represents production from B cells, the second term accounts for natural decay at rate δ_{pl}, and the third term represents the production of long-lived plasmocytes from memory B cells (at rate γ_{bm}).

Antibody Production: Finally, antibody production (A) is modeled by:

$$\frac{d}{dt}A = \pi_{AS}Ps + \pi_{AL}Pl - \delta_A A, \tag{12}$$

where π_{AS} and π_{AL} are the rates of antibody production by short- and long-lived plasmocytes, respectively, and δ_A is the natural decay rate of antibodies.

Table 1 presents the units for all constants used in our model (time is given in days).

Table 1. Units of the model constants (time is expressed in days).

Constant	Unit
$c_{v1}, \alpha_{Ap}, \beta_{Ap}, \delta_{Apm}, c_{11}, c_{14}, \alpha_{Tn}, \delta_{te}, \alpha_B, \delta_S, \delta_L, \gamma_M, k_{bm1}, \delta_A$	day^{-1}
c_{v2}, k_{ap2}	μg/mL
k_{v1}	$\frac{\text{mL}}{\mu\text{g}\cdot\text{day}}$
$k_{v2}, c_{12}, c_{13}, \pi_T, k_{te1}, \beta_S, \beta_L, \beta_{Bm}$	$\frac{\text{mL}}{\text{cells}\cdot\text{day}}$
k_{ap1}	Dimensionless
π_{B1}	$\frac{\text{mL}}{\mu\text{g}\cdot\text{day}}$
π_{B2}	$\frac{\text{mL}}{\text{cells}\cdot\text{day}}$
π_{AS}, π_{AL}	$\frac{\mu\text{g}}{\text{cells}\cdot\text{day}}$
k_{bm2}	cells/mL

4.2 Cohort Data

The cohort data were extracted from a phase 1, open-label, dose-escalation trial that evaluated the immunogenicity and reactogenicity of a type V GBS capsular polysaccharide-tetanus toxoid (TT) conjugate vaccine (V–TT). This was compared to an unconjugated type V capsular polysaccharide (V CPS) vaccine. The study included healthy men and non-pregnant women aged 18-50 years [1]. Sixty participants were randomly assigned to one of four vaccine groups, each receiving a single intramuscular dose:

- Unconjugated CPS: 37μg
- V–TT: 2.4μg CPS / 1.1μg TT
- V–TT: 9.6μg CPS / 4.3μg TT
- V–TT: 38.5μg CPS / 17.0μg TT

Blood samples were collected at baseline (pre-immunization) and at 4, 8, 26, and 52 weeks post-vaccination to assess humoral immune responses. Type V CPS-specific antibodies (IgG, IgA, and IgM) in serum samples were quantified using enzyme-linked immunosorbent assay (ELISA).

ICCS Camera Ready Version 2025
To cite this paper please use the final published version:
DOI: 10.1007/978-3-031-97554-7_27

4.3 Differential Evolution

Differential Evolution (DE) is an evolutionary algorithm introduced by Storn and Price in 1997 [21], renowned for its simplicity and efficiency in optimizing real-valued, multi-dimensional functions. As a population-based algorithm, DE employs mechanisms inspired by natural selection to iteratively refine candidate solutions. In our application, DE evolves a population of candidate solutions over successive generations to minimize an objective function, that is, the error between the antigen levels observed in the cohort data and those produced numerically.

Each candidate solution (or individual) is represented as a vector containing the adjustable parameter values within the search space. The core steps of the DE algorithm are mutation, crossover, and selection. Initially, a population of candidate solutions is generated randomly. For each candidate, a mutant vector is generated by combining three randomly selected individuals using differential mutation. Subsequently, a trial vector is formed by combining the mutant vector with the current candidate via a crossover operation. The trial vector replaces the current solution if it results in a lower objective function value, i.e., if it reduces the relative error between the antigen levels observed in the cohort data and those produced numerically. This relative error is computed using the L2 norm as follows:

$$R_E(A, \widehat{A}) = \|A(t) - \widehat{A}(t)\|_2, \tag{13}$$

where $A(t)$ represents the sum of IgM, IgG, and IgA levels from the cohort data, and $\widehat{A}(t)$ denotes the corresponding numerical value.

This process of mutation, crossover, and selection is repeated for a predefined number of generations or until a satisfactory solution is obtained.

Table 2 presents the adjustable constants and their respective intervals. These constants were selected based on a prior study, which identified them as the seven most sensitive parameters in the model [3]. The remaining constants and initial conditions are the same as in the original work [3].

Table 2. Constant bounds for model calibration.

Constant	Range
k_{v1}	$[1.0 \times 10^{-10},\ 1.0 \times 10^{1}]$
k_{v2}	$[1.0 \times 10^{-11},\ 1.0 \times 10^{4}]$
δ_{ps}	$[1.0 \times 10^{-6},\ 2.0 \times 10^{1}]$
α_{ap}	$[1.0 \times 10^{-6},\ 1.0 \times 10^{0}]$
β_{ap}	$[1.0 \times 10^{-6},\ 1.0 \times 10^{2}]$
δ_{apm}	$[1.0 \times 10^{-6},\ 1.0 \times 10^{0}]$
δ_A	$[1.0 \times 10^{-6},\ 1.0 \times 10^{0}]$

ICCS Camera Ready Version 2025
To cite this paper please use the final published version:
DOI: 10.1007/978-3-031-97554-7_27

5 Numerical Experiments

The numerical experiments were performed in two stages. First, we calibrated seven key constants (presented in Table 2) to cohort data using DE. This calibration was conducted for two vaccines: the unconjugated CPS vaccine and the V–TT vaccine at a dose of 9.6μg CPS/4.3μg TT.

Next, we simulated the immune response following the administration of the remaining two GBS vaccine doses. For these simulations, the initial conditions for vaccine and antibody levels were adjusted to match the values reported in the literature [1]. In particular, the initial vaccine values were computed based on an average blood volume of 5 liters. These initial condition values are presented in Table 3, while all other initial conditions were maintained as reported in the literature [3]. All other constants were set to the values obtained through DE calibration for the conjugated vaccine. This section presents the results of the numerical experiments.

Table 3. Initial conditions adopted in this work. All other conditions were kept the same as in the literature [3].

Dose	Vp	A
Unconjugated CPS	7.4×10^{-3}	1.0
V–TT: 2.4μg CPS / 1.1μg TT	7.0×10^{-4}	1.6
V–TT: 9.6μg CPS / 4.3μg TT	2.7×10^{-3}	1.3
V–TT: 38.5μg CPS / 17.0μg TT	1.11×10^{-2}	2.3

5.1 Computational Environment

The computational experiments were conducted on a machine equipped with dual AMD EPYC 7713 processors, providing a total of 128 physical cores. Each core features 64 KB of L1 data cache, 64 KB of L1 instruction cache, 512 KB of unified L2 cache, and shares a 32 MB L3 cache with seven other cores. The system ran GNU/Linux with kernel version 4.18.0-513.9.1.el8_9.

Despite the availability of many cores, the model was implemented sequentially. Python was used to develop the model, and the system of ODEs was numerically solved using the `odeint` function from the `scipy.integrate` package [13]. This function automatically selects an appropriate numerical method based on the characteristics of the ODE system, offering adaptive timesteps and convergence order. All experiments were performed using Python version 3.13.2.

5.2 Numerical Results and Discussion

The DE algorithm successfully calibrated seven key parameters to fit the model to the cohort data for both the unconjugated CPS vaccine (37μg) and the conjugated V–TT vaccine (9.6μg CPS/4.3μg TT), as shown in Figures 2A–B. The

ICCS Camera Ready Version 2025
To cite this paper please use the final published version:
DOI: 10.1007/978-3-031-97554-7_27

calibrated parameter values are presented in Table 4. Notably, significant differences were observed between the two vaccine formulations, reflecting their distinct immunological mechanisms.

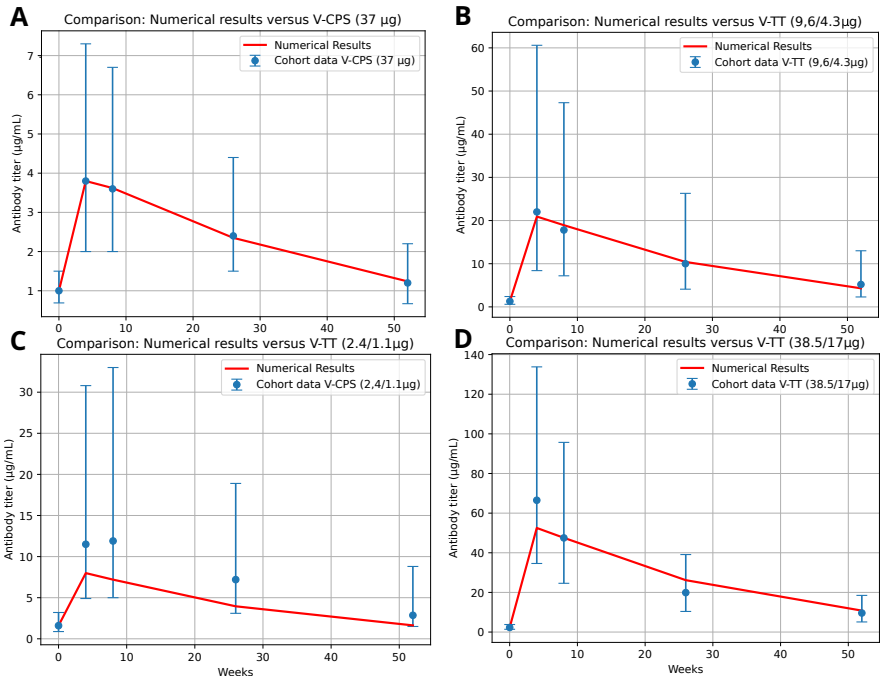

Fig. 2. Numerical results (red line) compared to GMT cohort data (blue dots) for four different GBS vaccines: (A) Unconjugated CPS: 37μg; (B) V-TT: 9.6μg CPS/4.3μg TT; (C) V-TT: 2.4μg CPS/1.1μg TT; and (D) V-TT: 38.5μg CPS/17.0μg TT. The numerical results for vaccines (A) and (B) were obtained after adjusting the seven model parameters in Table 2 using DE. The constant values obtained via DE (Table 4) were then used to simulate the other two vaccines (C and D) by modifying only the initial conditions (Table 3), to account for the distinct vaccine doses.

For the conjugated V–TT vaccine, the maturation rate of antigen-presenting cells (β_{ap}) was calibrated to a value 93 times higher than that of the unconjugated CPS vaccine (9.94×10^{-1} vs. 9.25×10^{1}). This aligns with the known adjuvant effect of tetanus toxoid, which enhances APC activation by promoting cross-talk between innate and adaptive immune systems [19]. Similarly, the innate-mediated vaccine clearance rate (k_{v1}) was approximately 1,700 times higher for the conjugated vaccine (3.15×10^{0} vs. 1.83×10^{-3}), suggesting that antibodies generated by the V–TT formulation more effectively neutralize vaccine particles, a hallmark of robust immunological memory that was also observed in opsonophagocytosis assays [1].

ICCS Camera Ready Version 2025
To cite this paper please use the final published version:
DOI: 10.1007/978-3-031-97554-7_27

The decay rate of short-lived plasmocytes (δ_{ps}) remained consistent between the two formulations (approximately 3.39×10^{0} to 3.91×10^{0} day^{-1}), indicating that short-term antibody production mechanisms are conserved regardless of conjugation. However, the antibody decay rate (δ_A) was slightly higher for the conjugated vaccine (3.41×10^{-2} vs. 2.47×10^{-2} day^{-1}), potentially reflecting faster antibody turnover due to increased immune activity.

Table 4. Constant values found after the calibration of the model.

Constant	Value for the Unconjugated CPS	Value for the V–TT 9.6μg CPS/4.3μg TT
k_{v1}	1.83×10^{-3}	3.15×10^{0}
k_{v2}	1.13×10^{-1}	6.07×10^{-1}
δ_{ps}	3.39×10^{0}	3.91×10^{0}
α_{ap}	5.92×10^{-1}	6.18×10^{-1}
β_{ap}	9.94×10^{-1}	9.25×10^{1}
δ_{apm}	8.36×10^{-1}	1.00×10^{0}
δ_A	2.47×10^{-2}	3.41×10^{-2}

Figure 2 compares simulated antibody titers to cohort data across four vaccine doses. The model accurately reproduced the dose-dependent response observed in the clinical trial, with higher CPS doses eliciting stronger and more sustained antibody levels.

The highest V–TT dose (38.5μg CPS/17.0μg TT) showed near-perfect alignment with cohort data, achieving a peak titer of approximately 50μg/mL at 8 weeks (Figure 2D). Lower doses (2.4μg CPS/1.1μg TT) exhibited greater discrepancies when compared with the other dosing regimens, with simulated titers consistently falling below the geometric mean titers (GMT) at all time points, albeit remaining within the confidence intervals. Although the model successfully replicated the overall dose-response trends, minor deviations at lower doses suggest opportunities for refinement. Incorporating additional parameters into the calibration process may further improve the model's precision.

6 Conclusions and Future Work

This study developed a computational model to simulate the immune response to the Type V GBS-TT conjugate vaccine, successfully reproducing clinical trial data across multiple dosages. By calibrating seven key parameters using Differential Evolution, the model captured the distinct immunological dynamics of both conjugated and unconjugated vaccines, providing mechanistic insights into their dose-dependent efficacy.

Our results, consistent with cohort data from the reference study, demonstrating that the conjugated V–TT vaccine elicits a more robust and sustained antibody response than the unconjugated CPS formulation. The numerical outcomes suggest that enhanced antigen-presenting cell (APC) maturation and ac-

ICCS Camera Ready Version 2025
To cite this paper please use the final published version:
DOI: 10.1007/978-3-031-97554-7_27

celerated antibody-mediated clearance—reflecting the adjuvant effect of tetanus toxoid—are critical factors driving this superior immune response.

Although the model aligned closely with cohort data for higher doses (e.g., 38.5μg CPS/17.0μg TT), minor discrepancies at lower doses (e.g., 2.4μg CPS/1.1μg TT) indicate opportunities for further refinement, such as incorporating additional parameters into the calibration process. Future work should also explore uncertainty quantification and consider integrating patient-specific immune profiles to enable personalized dosing recommendations, particularly for high-risk populations.

Acknowledgments. This work has been supported by UFJF, by CAPES - Finance Code 001; by CNPq - Grant number 308745/2021-3; by FAPEMIG Grant number APQ-02513-22; and by FINEP SOS Equipamentos 2021 AV02 0062/22.

Disclosure of Interests. The authors have no competing interests to declare that are relevant to the content of this article.

References

1. Baker, C.J., Rench, M.A., Paoletti, L.C., Edwards, M.S.: Dose–response to type V group B streptococcal polysaccharide–tetanus toxoid conjugate vaccine in healthy adults. Vaccine **25**(1), 55–63 (Jan 2007)
2. Benest, J., Rhodes, S., Evans, T.G., White, R.G.: Mathematical modelling for optimal vaccine dose finding: Maximising efficacy and minimising toxicity. Vaccines **10**(5), 756 (May 2022). https://doi.org/10.3390/vaccines10050756, http://dx.doi.org/10.3390/vaccines10050756
3. Bonin, C.R.B., Fernandes, G.C., de Menezes Martins, R., Camacho, L.A.B., Teixeira-Carvalho, A., da Mota, L.M.H., de Lima, S.M.B., Campi-Azevedo, A.C., Martins-Filho, O.A., dos Santos, R.W., Lobosco, M.: Validation of a yellow fever vaccine model using data from primary vaccination in children and adults, revaccination and dose-response in adults and studies with immunocompromised individuals. BMC Bioinformatics **21**(S17) (Dec 2020)
4. Bonin, C.R.B., Fernandes, G.C., dos Santos, R.W., Lobosco, M.: Mathematical modeling based on ordinary differential equations: A promising approach to vaccinology. Human Vaccines & Immunotherapeutics **13**(2), 484–489 (Dec 2016)
5. Bravi, B.: Development and use of machine learning algorithms in vaccine target selection. npj Vaccines **9**(1) (Jan 2024). https://doi.org/10.1038/s41541-023-00795-8, http://dx.doi.org/10.1038/s41541-023-00795-8
6. Castiglione, F., Liso, A.: The role of computational models of the immune system in designing vaccination strategies. Immunopharmacology and Immunotoxicology **27**(3), 417–432 (Jan 2005). https://doi.org/10.1080/08923970500241030, http://dx.doi.org/10.1080/08923970500241030
7. Folcik, V.A., An, G.C., Orosz, C.G.: The basic immune simulator: An agent-based model to study the interactions between innate and adaptive immunity. Theoretical Biology and Medical Modelling **4**(1) (Sep 2007). https://doi.org/10.1186/1742-4682-4-39, http://dx.doi.org/10.1186/1742-4682-4-39

ICCS Camera Ready Version 2025
To cite this paper please use the final published version:
DOI: 10.1007/978-3-031-97554-7_27

8. Hall, J., Adams, N.H., Bartlett, L., Seale, A.C., Lamagni, T., Bianchi-Jassir, F., Lawn, J.E., Baker, C.J., Cutland, C., Heath, P.T., Ip, M., Le Doare, K., Madhi, S.A., Rubens, C.E., Saha, S.K., Schrag, S., Sobanjo-ter Meulen, A., Vekemans, J., Gravett, M.G.: Maternal disease with group b streptococcus and serotype distribution worldwide: Systematic review and meta-analyses. Clinical Infectious Diseases **65**(Suppl 2), S112–S124 (Nov 2017)
9. Le, D., Miller, J.D., Ganusov, V.V.: Mathematical modeling provides kinetic details of the human immune response to vaccination. Frontiers in Cellular and Infection Microbiology **4** (Jan 2015). https://doi.org/10.3389/fcimb.2014.00177, http://dx.doi.org/10.3389/fcimb.2014.00177
10. Lee, E.K., Nakaya, H.I., Yuan, F., Querec, T.D., Burel, G., Pietz, F.H., Benecke, B.A., Pulendran, B.: Machine learning for predicting vaccine immunogenicity. Interfaces **46**(5), 368–390 (Oct 2016). https://doi.org/10.1287/inte.2016.0862, http://dx.doi.org/10.1287/INTE.2016.0862
11. Madrid, L., Seale, A.C., Kohli-Lynch, M., Edmond, K.M., Lawn, J.E., Heath, P.T., Madhi, S.A., Baker, C.J., Bartlett, L., Cutland, C., Gravett, M.G., Ip, M., Le Doare, K., Rubens, C.E., Saha, S.K., Sobanjo-ter Meulen, A., Vekemans, J., Schrag, S., Agarwal, R., da Silva, A.R.A., Bassat, Q., Berkley, J.A., Dangor, Z., Dhaded, S., Giannoni, E., Hammoud, M., Kobayahsi, M., O'Sullivan, C., Sakata, H., Sridhar, S., Sigaúque, B., Tyrrell, G., Paul, V.: Infant group b streptococcal disease incidence and serotypes worldwide: Systematic review and meta-analyses. Clinical Infectious Diseases **65**(Suppl 2), S160–S172 (Nov 2017)
12. Nuccitelli A, Rinaudo CD, M.D.: Group b streptococcus vaccine: state of the art. Ther Adv Vaccines **3**(3), 76–90 (2015). https://doi.org/10.1177/2051013615579869
13. Odeint: Odeint's homepage, accessed on october, 2020. (2020), http://docs.scipy.org
14. Pena, J.M.S., Lannes-Costa, P.S., Nagao, P.E.: Vaccines for streptococcus agalactiae: current status and future perspectives. Frontiers in Immunology **15** (2024). https://doi.org/10.3389/fimmu.2024.1430901
15. Pennisi, M., Russo, G., Ravalli, S., Pappalardo, F.: Combining agent based-models and virtual screening techniques to predict the best citrus-derived vaccine adjuvants against human papilloma virus. BMC Bioinformatics **18**(S16) (Dec 2017). https://doi.org/10.1186/s12859-017-1961-9, http://dx.doi.org/10.1186/s12859-017-1961-9
16. Raabe, V.N., Shane, A.L.: Group b streptococcus (streptococcus agalactiae). Microbiology Spectrum **7**(2) (Apr 2019). https://doi.org/10.1128/microbiolspec.gpp3-0007-2018, http://dx.doi.org/10.1128/microbiolspec.gpp3-0007-2018
17. Russell, N.J., Seale, A.C., O'Driscoll, M., O'Sullivan, C., Bianchi-Jassir, F., Gonzalez-Guarin, J., Lawn, J.E., Baker, C.J., Bartlett, L., Cutland, C., Gravett, M.G., Heath, P.T., Le Doare, K., Madhi, S.A., Rubens, C.E., Schrag, S., Sobanjo-ter Meulen, A., Vekemans, J., Saha, S.K., Ip, M., Asturias, E., Gaind, R., Kumar, P., Anthony, B., Madrid, L., Bassat, Q., Zhu, C., Luo, M., Nagarjuna, D., Majumder, S.: Maternal colonization with group b streptococcus and serotype distribution worldwide: Systematic review and meta-analyses. Clinical Infectious Diseases **65**(Suppl 2), S100–S111 (Nov 2017)
18. Seale, A.C., Blencowe, H., Bianchi-Jassir, F., Embleton, N., Bassat, Q., Ordi, J., Menéndez, C., Cutland, C., Briner, C., Berkley, J.A., Lawn, J.E., Baker, C.J., Bartlett, L., Gravett, M.G., Heath, P.T., Ip, M., Le Doare, K., Rubens, C.E., Saha, S.K., Schrag, S., Meulen, A.S.t., Vekemans, J., Madhi, S.A.: Stillbirth with

ICCS Camera Ready Version 2025
To cite this paper please use the final published version:
DOI: 10.1007/978-3-031-97554-7_27

group b streptococcus disease worldwide: Systematic review and meta-analyses. Clinical Infectious Diseases **65**(Suppl 2), S125–S132 (Nov 2017)
19. Siegrist, C.A.: Vaccine Immunology, pp. 16–34.e7. Elsevier (2018). https://doi.org/10.1016/b978-0-323-35761-6.00002-x, http://dx.doi.org/10.1016/B978-0-323-35761-6.00002-X
20. Sompayrac, L.: How the immune system works, sixth edition. The How it Works Series, Wiley-Blackwell, Hoboken, NJ, 6 edn. (Apr 2019)
21. Storn, R., Price, K.: Differential evolution – a simple and efficient heuristic for global optimization over continuous spaces. Journal of Global Optimization **11**(4), 341–359 (1997). https://doi.org/10.1023/a:1008202821328
22. Tomic, A., Tomic, I., Rosenberg-Hasson, Y., Dekker, C.L., Maecker, H.T., Davis, M.M.: Simon, an automated machine learning system, reveals immune signatures of influenza vaccine responses. The Journal of Immunology **203**(3), 749–759 (Aug 2019). https://doi.org/10.4049/jimmunol.1900033, http://dx.doi.org/10.4049/jimmunol.1900033
23. Xu, Z., Song, J., Zhang, H., Wei, Z., Wei, D., Yang, G., Demongeot, J., Zeng, Q.: A mathematical model simulating the adaptive immune response in various vaccines and vaccination strategies. Scientific Reports **14**(1) (Oct 2024). https://doi.org/10.1038/s41598-024-74221-x, http://dx.doi.org/10.1038/s41598-024-74221-x

ICCS Camera Ready Version 2025
To cite this paper please use the final published version:
DOI: 10.1007/978-3-031-97554-7_27